MOX–Report No. 48/2014

Effective governing equations for poroelastic growing media

Penta, R; Ambrosi, D; Shipley, R.

EFFECTIVE GOVERNING EQUATIONS FOR POROELASTIC GROWING MEDIA

by R. PENTA *and* D. AMBROSI

(*MOX-Dipartimento di Matematica, Politecnico di Milano, Piazza Leonardo da Vinci 32, 20133 Milano, Italy*)

R.J. SHIPLEY

(*Department of Mechanical Engineering, University College London, Torrington Place, London WC1E 7JE, United Kingdom*)

Summary

A new mathematical model is developed for the macroscopic behaviour of a porous, linear elastic solid, saturated with a slowly-flowing incompressible, viscous fluid, with surface accretion of the solid phase. The derivation uses a formal two-scale asymptotic expansion to exploit the well-separated length scales of the material: the pores are small compared to the macroscale, with a spatially-periodic microstructure. Surface accretion occurs at the interface between the solid and fluid phases, resulting in growth of the solid phase through mass exchange from the fluid at a prescribed rate (and *vice versa*). The averaging derives a new poroelastic model, which reduces to the classical result of Burridge and Keller in the limit of no growth. The new model is of relevance to a large range of applications including packed snow, tissue growth, biofilms and subsurface rocks or soils.

1. Introduction

The theory of poroelasticity concerns the mechanics of porous elastic solids with fluid-filled pores. The applications and motivations for this theory are far-reaching, and include the seepage of liquid waste disposed of underground, oil and gas recovery, soil consolidation and glaciers dynamics, as well as transport, mass exchange and solid stress in biological tissues. Whereas poroelasticity concerns fluid-solid interactions in two-phase materials, it lies within the broader field of mixture theory, which includes fluid and chemical transport in multiphase systems.

The literature in poroelasticity develops according to two main approaches; volume-averaging and homogenisation (the two are discussed in detail and compared in the review paper (**1**)). Most authors state *ab initio* the mass, momentum and energy balance equations for the individual phases on the basis of their "in bulk" mechanical behavior and utilize dissipation inequalities to restrict the possible constitutive equations for the components *in the mixture* (see (**2**) and (**3**)). While this approach allows for generality in the number of components and their mechanical nature, including finite elastic strains, any information on the microstructure of the material is suppressed by an implicit averaging procedure; as a consequence, effective coefficients that appear in the equations (for example, the fluid permeability) are at most characterized by their sign and are to be fitted by macroscopic experiments only.

The alternative homogenisation method exploits information on the geometry at the microscale by a multiscale expansion of the fields. This approach yields macroscopic equations with parameters that depend explicitly on the microscale geometry and physics; these parameters are obtained by averaging suitable microscale cell problems (as for example in (**4**), (**5**), (**6**) and (**7**)). The homogenisation technique is therefore powerful in retaining microscopic information; the drawback is that periodicity of the microstructure and linearity in the constitutive equations must be assumed. Moreover, the algebraic complexity of the method has reduced *de facto* its application to physical systems.

From the point of view of continuum mechanics, a challenging peculiarity of soft biological tissues is their ability to grow and remodel, a special characteristic of living matter that poses a number of intriguing mathematical questions: how to account for the resulting residual stress, which are the driving forces of growth, which are the corresponding regulatory mechanisms and the inner energy balance, see, e.g. (**8**), (**9**) and (**10**). This kind of questions has inspired a substantial body of literature in mathematical methods that, starting from one–component continuum mechanics, move towards the inclusion of multicomponent and microscale information in the model (**11**).

On the basis of the considerations above, it is not surprising that the specific issue of poroelastic materials that exchange mass has been mainly addressed in terms of mixtures, both for inert (see for example (**12**), (**13**) and (**14**)) and living matter (as in (**15**) and (**16**)). In the current study we seek to extend the existing poroelastic literature by considering mass exchange between elastic and fluid phases using a multiscale approach[†]. Although poroelasticity exhibits a wide range of applicability and growth is a crucial issue to address in a number of fields, the chief motivation for this work is biological. The growth and remodelling of living tissues is driven by chemical stimuli as well as the mechanical environment (alongside genetic cues) and the development of mathematical models that couple fluid and chemical transport with mechanical properties is of fundamental interest (as for example in (**15**) and (**16**)). A candidate system is a vascularised tissue, where the elastic phase (comprised of cells, fluid and protein matrix) undergoes small strains and the fluid phase (the blood supply) flows slowly. In this scenario, nutrients are delivered to the cell population by diffusion across the blood vessel walls, and may induce cellular proliferation and hence growth. In the context of drugs delivered through the blood supply, cellular death and tissue regression may result (for example, tumour treatment by chemotherapeutics); indeed, poroelastic frameworks have been used to model solid tumours (see (**17**), (**18**)) and the discussions within) and to extract tissue-specific poroelastic parameters from biological experiments (**19**). In a recent study (**20**), a combination of experiments and theory has also been used to develop a poroelastic model for the cytoplasm of living cells. Alternative scenarios of interest include tissue engineering applications, where tissue growth must be tightly controlled by providing a biomechanical and biochemical environment that mimics the physiological scenario. In many such situations surface growth of a cellular phase is a key feature, for example, in tissue expansion in hollow fibre bioreactors (**21**) (among many others). In (**22**), (**23**) and (**24**) mixture theory has been developed for such biological applications, and the interplay between fluid and chemical transport and tissue growth are explored; however, such models present challenges if the evolution of solid stresses are

---

[†] In this work we refer to interfacial mass exchange between the solid and the fluid phase as "growth", notwithstanding the sign of the mass flow that can actually indicate "resorption".

included (see (**25**) and (**11**) for examples and discussions). Also, a remarkable example of surface growth modelling can be found in (**26**), where a rigorous thermomechanical theory to account for the coupling between growth and mass transport phenomena across material interfaces is developed and biological examples are provided.

Inevitably any modelling approach faces challenges for integration with specific biological scenarios. Poroelastic materials (and, in general, multiphase frameworks) require the prescription of constitutive relationships to describe the fluid and solid stresses within the material of interest. In the case of linear elasticity, combined mathematical and experimental approaches (for example (**19**), (**20**)) have been used to extract solid parameters and make predictions around solid stress generation within living tissues. However, many biological soft tissues and cell aggregates behave as complex nonlinear-elastic (and possibly visco-plastic) materials, as in (**27**) and (**28**), so that the increased complexity of such models has limited the extraction of relevant parameters from biological experiments. Indeed, model parameterisation is a much broader issue given that mechanical, chemical and kinetic properties are both tissue and species-specific, and this motivates collaboration between biologists and mathematicians to close the data gap.

In the current study we derive a new poroelastic model that includes mass exchange between the solid and the fluid phase. The focus is on the accretion (or appositional growth) that occurs at the interface between solid and fluid in the pores. The mass exchange at the microscale interface modifies the mechanical properties of the elastic phase (which may be anisotropic) and the hydraulic characterization of the flow in the microstructure. While the small strains assumption applies to ensure linearity in the equations, finite growth (finite advancement of the fluid-solid interphase) is retained. This regime of infinitesimal displacement of the solid phase with respect to a finite evolution of the geometry rules out applicability of the model to questions of emergence of residual stress, an issue that should be addressed in the framework of nonlinear elasticity (**8**).

The model is derived using a two-scale asymptotic expansion, which exploits the separation between the length scale of the pores and the macroscale of the material. Such an approach has already been developed in the literature. In (**29**) Burridge and Keller present a rigorous derivation of Biot's equations of poroelasticity (see (**30**) and (**31**)) via the multiple scales method, whereas in (**32**) the interface law between a deformable porous medium containing a viscous fluid and an elastic body is derived using rigorous homogenisation and the two-scale convergence approach. In (**33**), Shipley and Chapman derive a dual porous medium model for vascular and interstitial fluid transport, and chemical transport, in a vascularised tissue. Here the averaging procedure is applied to a pore-scale description of coupled fluid transport and linear elasticity, with solid accretion at the interface between the two phases.

The paper is organized as follows. In section 2, we formulate the mechanical model description in both the fluid and solid phases of the material. The solid phase is described using a linear elastic model, and is coupled to Stokes' flow for the fluid phase via the normal component of stress on the interface between the two. Continuity of the mass flux is also imposed on the fluid-solid moving interface (**16**), alongside a growth law to describe its temporal evolution. In section 3 non-dimensionalisation of the equations is performed. Section 4 is devoted to the multiple scales analysis and, in particular, the assumptions of length scale separation and local periodicity are highlighted. Under these assumptions, a formal two-scale asymptotic expansion is used to decouple micro and macro

spatial variations, and thus derive the effective equations for a poroelastic growing material in section 5. The results are discussed in section 6, while in section 7 key limiting cases are highlighted; in particular the poroelastic equations of (**29**) are recovered in the limit of no growth, as well as the specific form of the model in the isotropic case. Finally, conclusions are presented in section 8.

2. The governing equations for a poroelastic growing medium

We consider a set $\Omega \in \mathbb{R}^3$, such that $\Omega = \Omega_s \cup \Omega_f$, where Ω_s and Ω_f represent the porous solid and fluid compartment, respectively. At this stage, every field of interest is a function of space $\boldsymbol{x}$ and time t. We assume the typical length scale r of the pores to be small compared to the characteristic size d of the domain (see Fig. 1), so that their ratio

$$\frac{r}{d} = \epsilon \ll 1. \tag{2.1}$$

We consider an incompressible Newtonian fluid, so that, assuming that body forces and inertial effects can be neglected, the Stokes' problem holds in the fluid domain Ω_f:

$$\nabla \cdot \sigma = 0 \tag{2.2}$$
$$\nabla \cdot \boldsymbol{v} = 0,$$

where σ denotes the fluid stress tensor defined by

$$\sigma = -p\mathsf{I} + \mu \left(\nabla \boldsymbol{v} + (\nabla \boldsymbol{v})^\mathsf{T} \right) \tag{2.3}$$

and $\boldsymbol{v}$, p, μ are the fluid velocity, pressure and viscosity respectively.

The solid phase is modelled as a linear, elastic solid, with inertia and body forces neglected, through

$$\nabla \cdot \tau = 0 \tag{2.4}$$

in Ω_s, where the solid stress tensor τ is given by

$$\tau = \mathbb{C}\nabla \boldsymbol{u}. \tag{2.5}$$

Here, $\boldsymbol{u}$ is the displacement vector for the solid compartment and $\mathbb{C}$ is the fourth rank elasticity tensor (with components denoted C_{ijkl} for $i, j, k, l = 1, 2, 3$), completely defined by its action on the symmetric part of $\nabla \boldsymbol{u}$ (see, e.g. (**34**)), through:

$$\mathbb{C}\nabla \boldsymbol{u} = \mathbb{C}\mathsf{e}, \tag{2.6}$$
$$\mathsf{e} := \frac{\nabla \boldsymbol{u} + (\nabla \boldsymbol{u})^\mathsf{T}}{2}.$$

In other words, the skew component of $\nabla \boldsymbol{u}$ is in the kernel of $\mathbb{C}$. Note that if $\mathbb{C}\nabla \boldsymbol{u} = \mathbb{C}\mathsf{e} = 0$ then $\boldsymbol{u}$ is a rigid body motion.

Interface conditions for the fluid-structure interaction apply between the fluid and the solid phase. Following (**16**), the boundary $\Gamma := \partial\Omega_s \cap \partial\Omega_f$ is represented as a moving interface with velocity $\boldsymbol{v}_\Gamma$. Enforcing global mass conservation in Ω we define:

$$\rho_f(\boldsymbol{v} - \boldsymbol{v}_\Gamma) \cdot \boldsymbol{n} = \rho_s(\dot{\boldsymbol{u}} - \boldsymbol{v}_\Gamma) \cdot \boldsymbol{n} = \tilde{g} \quad \text{on } \Gamma, \tag{2.7}$$

where $\dot{\boldsymbol{u}}$, ρ_f and ρ_s are the solid phase velocity and the fluid and solid densities, respectively. Here $\boldsymbol{n}$ is the unit vector normal to the interface pointing into the solid region, and $\tilde{g}$ is the mass transfer rate per unit of surface area, which is assumed to be prescribed and strictly positive in the case of solid phase growth. Equation (2.7) accounts for mass exchange between the solid and fluid phase, and is equivalent to the following two scalar conditions:

$$\rho_s(\dot{\boldsymbol{u}} - \boldsymbol{v}_\Gamma) \cdot \boldsymbol{n} = \tilde{g} \quad \text{on } \Gamma, \tag{2.8}$$

$$\rho_f(\boldsymbol{v} - \boldsymbol{v}_\Gamma) \cdot \boldsymbol{n} = \tilde{g} \quad \text{on } \Gamma. \tag{2.9}$$

Equations (2.8, 2.9) relate the interface velocity to the mass transfer rate $\tilde{g}$ and to the solid and fluid velocities and densities, respectively. From (2.8) we obtain:

$$\boldsymbol{v}_\Gamma \cdot \boldsymbol{n} = \dot{\boldsymbol{u}} \cdot \boldsymbol{n} - \frac{\tilde{g}}{\rho_s} \quad \text{on } \Gamma. \tag{2.10}$$

Substituting (2.10) into equation (2.9) gives:

$$\rho_f \boldsymbol{v} \cdot \boldsymbol{n} - \rho_f \dot{\boldsymbol{u}} \cdot \boldsymbol{n} + \rho_f \frac{\tilde{g}}{\rho_s} = \tilde{g} \quad \text{on } \Gamma. \tag{2.11}$$

Finally, dividing by ρ_f and rearranging terms, equation (2.11) yields the following jump condition for the fluid and solid velocities at the interface:

$$(\boldsymbol{v} - \dot{\boldsymbol{u}}) \cdot \boldsymbol{n} = \tilde{g}\left(\frac{1}{\rho_f} - \frac{1}{\rho_s}\right) \quad \text{on } \Gamma. \tag{2.12}$$

In order to simplify notation, we denote by g the right hand side of (2.12), so that

$$g := \tilde{g}\left(\frac{1}{\rho_f} - \frac{1}{\rho_s}\right). \tag{2.13}$$

The tangential components of the velocity and all components of the stress on Γ are continuous across the interface, such that

$$\tau\boldsymbol{n} = \sigma\boldsymbol{n} \qquad \text{on } \Gamma \tag{2.14}$$
$$\dot{\boldsymbol{u}} \cdot \boldsymbol{t} = \boldsymbol{v} \cdot \boldsymbol{t} \qquad \text{on } \Gamma, \tag{2.15}$$

where $\boldsymbol{t}$ is any unit vector tangent to the interface.

2.1 *Kinematics of the moving interface*
The interface velocity (which is directed along $\boldsymbol{n}$), satisfies

$$\boldsymbol{v}_\Gamma \cdot \boldsymbol{n} = \boldsymbol{v} \cdot \boldsymbol{n} - \frac{\tilde{g}}{\rho_f} = \dot{\boldsymbol{u}} \cdot \boldsymbol{n} - \frac{\tilde{g}}{\rho_s}, \tag{2.16}$$

where equations (2.8, 2.9) have been used for the simplification. The function $\tilde{g}$ accounts for surface growth and should be constitutively specified according to the physical system at hand. We further note that, as the interface is moving, the fluid and solid subdomains

$\Omega_s(t)$ and $\Omega_f(t)$ change in time [†]. The assumptions underlying the material descriptions of the solid and fluid phases (small deformation of the solid elastic phase, negligible inertia) do not affect surface growth. The present framework allows for finite growth at a pore scale; the position of the fluid-solid interface evolves in time according to the interface velocity condition (2.16), and global mass conservation in Ω is ensured by the jump condition (2.12). Assuming that the moving interface is described by $F(\boldsymbol{x}, t) = 0$, its kinematics are described by:

$$\frac{\partial F}{\partial t} + \nabla F \cdot \boldsymbol{v}_\Gamma = 0. \tag{2.17}$$

Equations (2.2-2.5) describing the mechanics of the fluid and solid phases, together with the interface conditions (2.12, 2.14, 2.15) and the kinematic relationships for the evolution of the interface (2.16–2.17), represent the system of partial differential equations to be solved for every $\boldsymbol{x} \in \Omega$ and for every $t \in (0, T)$, $T \in \mathbb{R}^+$, (subject to appropriate initial and boundary conditions). When $\tilde{g} = 0$, there is no growth and the normal components of the fluid and solid velocities are equal and are the velocity of the interface itself. In this particular case the problem reduces to a standard linearized fluid-structure interaction problem as in (**29**).

3. Non-dimensionalisation

Next we formulate the model in non-dimensional form in order to clarify the mutual weight of the relevant physical mechanisms. The model derived in this paper does not aim to be application-specific; as such, we do not motivate the non-dimensionalisation via specific parameter values (see, e.g. (**33**) and (**35**) for biological tissues), but instead we perform a formal non-dimensionalisation to highlight the proper asymptotic behaviour of the relevant fields. We rescale

$$\boldsymbol{x} = d\boldsymbol{x}', \quad \boldsymbol{v} = \frac{Cr^2}{\mu_c}\boldsymbol{v}', \quad \boldsymbol{v}_\Gamma = \frac{Cr^2}{\mu_c}\boldsymbol{v}'_\Gamma \quad p = Cdp', \quad \boldsymbol{u} = d\boldsymbol{u}', \quad t = \frac{d\mu_c}{Cr^2}t',$$

$$\tilde{g} = \rho_c\frac{Cr^2}{\mu_c}\tilde{g}', \quad \mu = \mu_c\mu', \quad \rho_s = \rho_c\rho'_s, \quad \rho_f = \rho_c\rho'_f, \quad \mathbb{C} = Cd\mathbb{C}',$$

$$g = \frac{Cr^2}{\mu_c}g', \quad g' = \tilde{g}'\left(\frac{1}{\rho'_f} - \frac{1}{\rho'_s}\right), \quad \tau = Cd\tau', \quad \sigma = Cd\sigma', \tag{3.1}$$

where C, ρ_c, μ_c denote the characteristic pressure gradient, density and viscosity, respectively. Here, we scale the spatial coordinate and the elastic displacement by the characteristic length scale of the domain d, whereas the non–dimensional form of the velocity is suggested by the parabolic profile of a viscous fluid flowing in a straight channel of radius r

$$V = \frac{Cr^2}{\mu_c}. \tag{3.2}$$

Further, we scale pressure and stresses by adopting the same reference pressure gradient exploited in (3.2), (multiplied by the reference length scale d) and time assuming d/V as a reference time scale for slow flow of the fluid phase (which is analogous to that for deformation of the elastic material).

[†] We avoid denoting this time dependence explicitly in the following sections for simplicity of notation

Thus, exploiting (3.1) and dropping the prime notation for the sake of simplicity, equations (2.2-2.5), (2.12, 2.14, 2.15) become:

$$\nabla \cdot \sigma = 0 \qquad \text{in } \Omega_f \qquad (3.3)$$

$$-p\mathsf{I} + \epsilon^2 \mu \left(\nabla \boldsymbol{v} + (\nabla \boldsymbol{v})^{\mathsf{T}} \right) = \sigma \qquad \text{in } \Omega_f \qquad (3.4)$$

$$\nabla \cdot \boldsymbol{v} = 0 \qquad \text{in } \Omega_f \qquad (3.5)$$

$$\tau \boldsymbol{n} = \sigma \boldsymbol{n} \qquad \text{on } \Gamma \qquad (3.6)$$

$$(\boldsymbol{v} - \dot{\boldsymbol{u}}) \cdot \boldsymbol{n} = g \qquad \text{on } \Gamma \qquad (3.7)$$

$$\dot{\boldsymbol{u}} \cdot \boldsymbol{t} = \boldsymbol{v} \cdot \boldsymbol{t} \quad \text{on } \Gamma \qquad (3.8)$$

$$\nabla \cdot \tau = 0 \qquad \text{in } \Omega_s \qquad (3.9)$$

$$\mathbb{C} \nabla \boldsymbol{u} = \tau \qquad \text{in } \Omega_s. \qquad (3.10)$$

The ϵ^2 coefficient that appears in (3.4) follows when assuming a reference velocity of the type (3.2) and is the standard scaling for Stokes' flow in porous media (see for example (**4**), (**6**), (**29**), and (**36**)), which reflects the asymptotic behaviour of the characteristic fluid velocity in the pores, that scales with ϵ^2 as $\epsilon \to 0$, as noted in (**5**).

The kinematic condition is rewritten in non–dimensional form using the pore spatial scale r, so that the relevant time scale is

$$T_g = \frac{r}{V} = \epsilon \frac{d\mu_c}{Cr^2}. \qquad (3.11)$$

The interface kinematic equations (2.16, 2.17) with the time scale (3.11) yields, in non–dimensional form

$$\frac{1}{\epsilon} \frac{\partial F}{\partial t} + \nabla F \cdot \boldsymbol{v}_\Gamma = 0, \qquad (3.12)$$

$$\boldsymbol{v}_\Gamma \cdot \boldsymbol{n} = \boldsymbol{v} \cdot \boldsymbol{n} - \frac{\tilde{g}}{\rho_f} = \dot{\boldsymbol{u}} \cdot \boldsymbol{n} - \frac{\tilde{g}}{\rho_s}, \qquad (3.13)$$

where the prime notation has again been neglected, and the ϵ^{-1} term appearing at the left hand side of (3.12) accounts for the time scale separation between finite growth and linearized motion of the material.

4. Multiple scales formulation

In this section we employ a formal two-scales asymptotic expansion widely exploited in the literature (for example (**4**), (**5**), (**6**), (**7**) and (**37**)) to derive a continuum macroscale model for the system of equations (3.3-3.10, 3.12-3.13). Since $\epsilon \ll 1$, we enforce a sharp length scale separation between r (the *microscale*) and d (the *macroscale*), defining:

$$\boldsymbol{y} := \frac{\boldsymbol{x}}{\epsilon}. \qquad (4.1)$$

Following the usual approach in multiscale analysis, from now on $\boldsymbol{x}$ and $\boldsymbol{y}$ denote independent variables, representing the macro and micro spatial scale, respectively. In

the analysis that follows, all the fields (denoted collectively by ψ) and the elasticity tensor $\mathbb{C}$ are functions of these independent spatial variables:

$$\psi = \psi(\boldsymbol{x}, \boldsymbol{y}, t), \quad \mathbb{C} = \mathbb{C}(\boldsymbol{x}, \boldsymbol{y}),$$

and the differential operators transform accordingly,

$$\nabla \to \nabla_{\boldsymbol{x}} + \frac{1}{\epsilon}\nabla_{\boldsymbol{y}}. \tag{4.2}$$

Now we formally perform the following multiple scales expansion in power series of ϵ for every field ψ:

$$\psi_\epsilon(\boldsymbol{x}, \boldsymbol{y}, t) = \sum_{l=0}^{\infty} \psi^{(l)}(\boldsymbol{x}, \boldsymbol{y}, t)\epsilon^l. \tag{4.3}$$

The components $\psi^{(l)}$ are defined for every $\boldsymbol{x}$ belonging to the macroscale domain, whereas $\boldsymbol{y}$ spans only the specific portion of the microscale where ψ is defined. We further assume regularity of the microstructure, so that every $\psi^{(l)}$ and $\mathbb{C}$ are $\boldsymbol{y}$-periodic. This means that *local* periodicity only is assumed, such that any (regular enough) macroscale variation in any field ψ is in principle allowed. Furthermore, since the surface description F can macroscopically vary, macroscale variations in the interface Γ are also permitted. A schematic of the setup is shown in Figure 1.
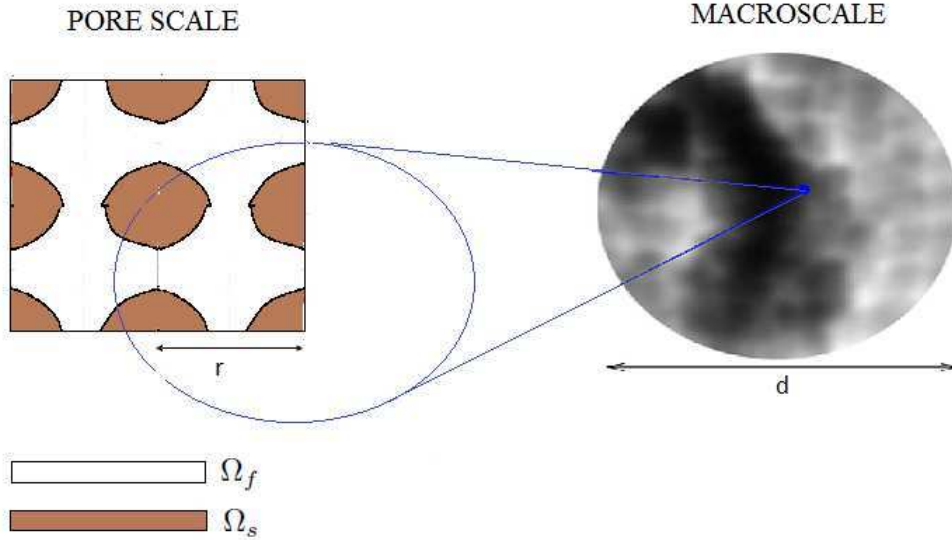
Fig. 1 A 2D cartoon of the pore scale (left), depicting the porous structure of the medium on the microscale and the corresponding *homogenised* one on the macroscale (right), where the geometry of the microstructure is smoothed out.

Under the transformation (4.2), equations (3.3-3.10, 3.12-3.13) become:

$$\nabla_{\boldsymbol{y}} \cdot \sigma_\epsilon + \epsilon \nabla_{\boldsymbol{x}} \cdot \sigma_\epsilon = 0 \qquad \text{in } \Omega_f \qquad (4.4)$$

$$p_\epsilon \mathsf{I} - \epsilon \mu \left(\nabla_{\boldsymbol{y}} \boldsymbol{v}_\epsilon + (\nabla_{\boldsymbol{y}} \boldsymbol{v}_\epsilon)^\mathsf{T} \right) - \epsilon^2 \mu \left(\nabla_{\boldsymbol{x}} \boldsymbol{v}_\epsilon + (\nabla_{\boldsymbol{x}} \boldsymbol{v}_\epsilon)^\mathsf{T} \right) = \sigma_\epsilon \qquad \text{in } \Omega_f \qquad (4.5)$$

$$\nabla_{\boldsymbol{y}} \cdot \boldsymbol{v}_\epsilon + \epsilon \nabla_{\boldsymbol{x}} \cdot \boldsymbol{v}_\epsilon = 0 \qquad \text{in } \Omega_f \qquad (4.6)$$

$$\tau_\epsilon \boldsymbol{n} = \sigma_\epsilon \boldsymbol{n} \qquad \text{on } \Gamma \qquad (4.7)$$

$$\dot{\boldsymbol{u}}_\epsilon \cdot \boldsymbol{t} = \boldsymbol{v}_\epsilon \cdot \boldsymbol{t} \qquad \text{on } \Gamma \qquad (4.8)$$

$$\boldsymbol{v}_\epsilon \cdot \boldsymbol{n} - \dot{\boldsymbol{u}}_\epsilon \cdot \boldsymbol{n} = g_\epsilon \qquad \text{on } \Gamma \qquad (4.9)$$

$$\nabla_{\boldsymbol{y}} \cdot \tau_\epsilon + \epsilon \nabla_{\boldsymbol{x}} \cdot \tau_\epsilon = 0 \qquad \text{in } \Omega_s \qquad (4.10)$$

$$\frac{1}{\epsilon} \mathbb{C} \nabla_{\boldsymbol{y}} \boldsymbol{u}_\epsilon + \mathbb{C} \nabla_{\boldsymbol{x}} \boldsymbol{u}_\epsilon = \tau_\epsilon \qquad \text{in } \Omega_s \qquad (4.11)$$

$$\frac{\partial F_\epsilon}{\partial t} + \nabla_{\boldsymbol{y}} F_\epsilon \cdot \boldsymbol{v}_{\Gamma\epsilon} + \epsilon \nabla_{\boldsymbol{x}} F_\epsilon \cdot \boldsymbol{v}_{\Gamma\epsilon} = 0 \qquad (4.12)$$

$$\boldsymbol{v}_{\Gamma\epsilon} \cdot \boldsymbol{n} = \boldsymbol{v}_\epsilon \cdot \boldsymbol{n} - \frac{\tilde{g}_\epsilon}{\rho_f} = \dot{\boldsymbol{u}}_\epsilon \cdot \boldsymbol{n} - \frac{\tilde{g}_\epsilon}{\rho_s} \quad \text{on } \Gamma, \qquad (4.13)$$

where p_ϵ, $\boldsymbol{v}_\epsilon$, $\boldsymbol{u}_\epsilon$, σ_ϵ, τ_ϵ, $\boldsymbol{v}_{\Gamma\epsilon}$, $\tilde{g}_\epsilon$, g_ϵ, F_ϵ are the representation in the power series form (4.3) of the corresponding fields. Next we substitute power series expansions of the form (4.3) into the relevant fields in (4.4-4.13); by equating coefficients of ϵ^l for $l = 0, 1, ...$, we derive the macroscale model for the poroelastic growing medium in terms of the leading (zero-th) order relevant fields.

5. The macroscopic model

In this section we derive a closed system of partial differential equations for the macroscopic behaviour of the leading order fields $p^{(0)}$, $\boldsymbol{v}^{(0)}$, $\boldsymbol{u}^{(0)}$, by averaging over the zero-th and first order systems corresponding to (4.4–4.13) .

Whenever a component of the asymptotic expansion retains a dependence on the microscale $\boldsymbol{y}$, we can take its integral average, defined as follows:

$$\langle \psi \rangle_k = \frac{1}{|\Omega|} \int_{\Omega_k} \psi(\boldsymbol{x}, \boldsymbol{y}, t) \, \mathrm{d}\boldsymbol{y} \quad k = f, s, \qquad (5.1)$$

where $|\Omega|$ represents the volume of the domain and integration is performed over the microscale $\boldsymbol{y}$. Because of $\boldsymbol{y}$-periodicity, the integral average can be performed over one representative cell only (see Figure 1): from now on, (5.1) should be understood as a cell average, where $|\Omega|$ is replaced by the cell volume and Ω_k by the corresponding k-phase subvolume.

Equating coefficients of ϵ^0 in the system (4.4-4.13) yields:

$$\nabla_{\boldsymbol{y}} \cdot \sigma^{(0)} = 0 \qquad\qquad \text{in } \Omega_f \qquad (5.2)$$

$$\sigma^{(0)} = -p^{(0)}\mathsf{I} \qquad\qquad \text{in } \Omega_f \qquad (5.3)$$

$$\nabla_{\boldsymbol{y}} \cdot \boldsymbol{v}^{(0)} = 0 \qquad\qquad \text{in } \Omega_f \qquad (5.4)$$

$$\tau^{(0)}\boldsymbol{n} = \sigma^{(0)}\boldsymbol{n} \qquad\qquad \text{on } \Gamma \qquad (5.5)$$

$$\dot{\boldsymbol{u}}^{(0)} \cdot \boldsymbol{t} = \boldsymbol{v}^{(0)} \cdot \boldsymbol{t} \qquad\qquad \text{on } \Gamma \qquad (5.6)$$

$$\boldsymbol{v}^{(0)} \cdot \boldsymbol{n} - \dot{\boldsymbol{u}}^{(0)} \cdot \boldsymbol{n} = g^{(0)} \qquad\qquad \text{on } \Gamma \qquad (5.7)$$

$$\nabla_{\boldsymbol{y}} \cdot \tau^{(0)} = 0 \qquad\qquad \text{in } \Omega_s \qquad (5.8)$$

$$\mathbb{C}\nabla_{\boldsymbol{y}}\boldsymbol{u}^{(0)} = 0 \qquad\qquad \text{in } \Omega_s \qquad (5.9)$$

$$\frac{\partial F^{(0)}}{\partial t} + \nabla_{\boldsymbol{y}} F^{(0)} \cdot \boldsymbol{v}_{\Gamma}^{(0)} = 0 \qquad\qquad (5.10)$$

$$\boldsymbol{v}_{\Gamma}^{(0)} \cdot \boldsymbol{n} = \boldsymbol{v}^{(0)} \cdot \boldsymbol{n} - \frac{\tilde{g}^{(0)}}{\rho_f} = \dot{\boldsymbol{u}}^{(0)} \cdot \boldsymbol{n} - \frac{\tilde{g}^{(0)}}{\rho_s} \qquad\qquad \text{on } \Gamma, \qquad (5.11)$$

whereas equating coefficients of ϵ^1 in equations (4.4-4.11) yields

$$\nabla_{\boldsymbol{y}} \cdot \sigma^{(1)} + \nabla_{\boldsymbol{x}} \cdot \sigma^{(0)} = 0 \qquad\qquad \text{in } \Omega_f \qquad (5.12)$$

$$-p^{(1)}\mathsf{I} + \mu\left(\nabla_{\boldsymbol{y}}\boldsymbol{v}^{(0)} + \left(\nabla_{\boldsymbol{y}}\boldsymbol{v}^{(0)}\right)^{\mathsf{T}}\right) = \sigma^{(1)} \qquad\qquad \text{in } \Omega_f \qquad (5.13)$$

$$\nabla_{\boldsymbol{y}} \cdot \boldsymbol{v}^{(1)} + \nabla_{\boldsymbol{x}} \cdot \boldsymbol{v}^{(0)} = 0 \qquad\qquad \text{in } \Omega_f \qquad (5.14)$$

$$\tau^{(1)}\boldsymbol{n} = \sigma^{(1)}\boldsymbol{n} \qquad\qquad \text{on } \Gamma \qquad (5.15)$$

$$\dot{\boldsymbol{u}}^{(1)} \cdot \boldsymbol{t} = \boldsymbol{v}^{(1)} \cdot \boldsymbol{t} \qquad\qquad \text{on } \Gamma \qquad (5.16)$$

$$\boldsymbol{v}^{(1)} \cdot \boldsymbol{n} - \dot{\boldsymbol{u}}^{(1)} \cdot \boldsymbol{n} = g^{(1)} \qquad\qquad \text{on } \Gamma \qquad (5.17)$$

$$\nabla_{\boldsymbol{y}} \cdot \tau^{(1)} + \nabla_{\boldsymbol{x}} \cdot \tau^{(0)} = 0 \qquad\qquad \text{in } \Omega_s \qquad (5.18)$$

$$\mathbb{C}\left(\nabla_{\boldsymbol{y}}\boldsymbol{u}^{(1)} + \nabla_{\boldsymbol{x}}\boldsymbol{u}^{(0)}\right) = \tau^{(0)} \qquad\qquad \text{in } \Omega_s. \qquad (5.19)$$

Equations (5.2-5.3) infer that $p^{(0)}$ does not depend on the microscale $\boldsymbol{y}$, hence

$$p^{(0)} = p^{(0)}(\boldsymbol{x}, t). \qquad\qquad (5.20)$$

Equation (5.9) implies, together with the elasticity tensor property (2.6), that $\boldsymbol{u}^{(0)}$ must correspond to a rigid body motion. Since the only $\boldsymbol{y}$-periodic solution of this type is $\boldsymbol{y}$-constant, we see that:

$$\boldsymbol{u}^{(0)} = \boldsymbol{u}^{(0)}(\boldsymbol{x}, t). \qquad\qquad (5.21)$$

Hence the leading order solid displacement field is also locally constant.

5.1 *Macroscale fluid flow*

In order to obtain information on the leading order velocity of the fluid $\boldsymbol{v}^{(0)}$, we note that, enforcing (5.3), equations (5.6-5.7,5.12-5.13) form a Stokes-type boundary value problem

for $(\boldsymbol{v}^{(0)}, p^{(1)})$ which can be rewritten in terms of the relative fluid-solid displacement $\boldsymbol{w}$ defined by:

$$\dot{\boldsymbol{w}}(\boldsymbol{x}, \boldsymbol{y}, t) := \boldsymbol{v}^{(0)}(\boldsymbol{x}, \boldsymbol{y}, t) - \dot{\boldsymbol{u}}^{(0)}(\boldsymbol{x}, t), \tag{5.22}$$

as follows:

$$\mu \nabla_{\boldsymbol{y}}^2 \dot{\boldsymbol{w}} - \nabla_{\boldsymbol{y}} p^{(1)} - \nabla_{\boldsymbol{x}} p^{(0)} = 0 \qquad \text{in } \Omega_f \tag{5.23}$$

$$\nabla_{\boldsymbol{y}} \cdot \dot{\boldsymbol{w}} = 0 \qquad \text{in } \Omega_f \tag{5.24}$$

$$\dot{\boldsymbol{w}} \cdot \boldsymbol{t} = 0 \qquad \text{on } \Gamma \tag{5.25}$$

$$\dot{\boldsymbol{w}} \cdot \boldsymbol{n} = g^{(0)} \qquad \text{on } \Gamma, \tag{5.26}$$

where the knowledge that $\boldsymbol{u}^{(0)}$ is locally constant has been explicitly used. Now we exploit linearity together with (5.20) and propose the following ansatz for the solution $(\dot{\boldsymbol{w}}, p^{(1)})$:

$$\dot{\boldsymbol{w}} = -\tilde{\mathsf{W}} \nabla_{\boldsymbol{x}} p^{(0)} + \boldsymbol{h}, \tag{5.27}$$

$$p^{(1)} = -\boldsymbol{P} \cdot \nabla_{\boldsymbol{x}} p^{(0)} + p_h, \tag{5.28}$$

where $p^{(1)}$ is defined up to an arbitrary $\boldsymbol{y}$-constant function and the quantities $(\tilde{\mathsf{W}}, \boldsymbol{P})$, $(\boldsymbol{h}, p_h)$ satisfy the following differential *cell problems*, to be solved on the single representative cell

$$\mu \nabla_{\boldsymbol{y}}^2 \tilde{\mathsf{W}}^\mathsf{T} - \nabla_{\boldsymbol{y}} \boldsymbol{P} + \mathsf{I} = 0 \quad \text{in } \Omega_f \tag{5.29}$$

$$\nabla_{\boldsymbol{y}} \cdot \tilde{\mathsf{W}}^\mathsf{T} = 0 \quad \text{in } \Omega_f \tag{5.30}$$

$$\tilde{\mathsf{W}} = 0 \quad \text{on } \Gamma, \tag{5.31}$$

$$\mu \nabla_{\boldsymbol{y}}^2 \boldsymbol{h} - \nabla_{\boldsymbol{y}} p_h = 0 \qquad \text{in } \Omega_f \tag{5.32}$$

$$\nabla_{\boldsymbol{y}} \cdot \boldsymbol{h} = 0 \qquad \text{in } \Omega_f \tag{5.33}$$

$$\boldsymbol{h} \cdot \boldsymbol{t} = 0 \qquad \text{on } \Gamma \tag{5.34}$$

$$\boldsymbol{h} \cdot \boldsymbol{n} = g^{(0)} \qquad \text{on } \Gamma. \tag{5.35}$$

The above system of equations (5.29–5.31) and (5.32–5.35) are supplemented by periodicity conditions on the unit cell in $\boldsymbol{y}$, together with suitable uniqueness conditions for $\boldsymbol{P}$, p_h. Example conditions are

$$\langle \boldsymbol{P} \rangle_f = \boldsymbol{0}, \quad \langle p_h \rangle_f = 0. \tag{5.36}$$

Exploiting definition (5.22) and equation (5.27), we notice that $\boldsymbol{v}^{(0)}$, and hence its cell average, can be recovered in terms of $p^{(0)}$ and $\boldsymbol{u}^{(0)}$ as follows:

$$\langle \dot{\boldsymbol{w}} \rangle_f = \left\langle \boldsymbol{v}^{(0)} \right\rangle_f - \phi \dot{\boldsymbol{u}}^{(0)} = - \left\langle \tilde{\mathsf{W}} \right\rangle_f \nabla_{\boldsymbol{x}} p^{(0)} + \langle \boldsymbol{h} \rangle_f, \tag{5.37}$$

where

$$\phi(\boldsymbol{x}, t) := \frac{|\Omega_f|}{|\Omega|} \tag{5.38}$$

is the porosity of the material.

Remark 5.1. Exploiting the local incompressibility constraint (5.33) together with interface condition (5.35) and $\boldsymbol{y}$-periodicity, we note that:

$$0 = \int_{\Omega_f} \nabla_{\boldsymbol{y}} \cdot \boldsymbol{h} \, \mathrm{d}\boldsymbol{y} = \int_{\partial \Omega_f} \boldsymbol{h} \cdot \boldsymbol{n} \, \mathrm{d}S_y = \int_{\Gamma} \boldsymbol{h} \cdot \boldsymbol{n} \, \mathrm{d}S_y = \int_{\Gamma} g^{(0)} \, \mathrm{d}S_y. \qquad (5.39)$$

Hence, the cell problem (5.32-5.35) has a solution if and only if the compatibility condition

$$\int_{\Gamma} g^{(0)} \, \mathrm{d}S_y = 0 \qquad (5.40)$$

is satisfied. Given that

$$g^{(0)} = \tilde{g}^{(0)} \left(\frac{1}{\rho_f} - \frac{1}{\rho_s} \right), \qquad (5.41)$$

and $\tilde{g}^{(0)} \neq 0$ when surface growth is occurring, condition (5.40) is automatically satisfied whenever the density difference between the fluid and solid compartment is negligible,

$$\rho_f = \rho_s. \qquad (5.42)$$

In this case, every $g^{(l)}$ for $l = 0, 1, \dots$ and in particular $g^{(0)}$ reduces to zero and the unique solution of the cell problem (5.32-5.35) is $\boldsymbol{h} = \boldsymbol{0}$. This is not surprising, as the interface condition (5.35) is directly related to the jump condition (5.26), that arises from mass conservation for a moving interface. Indeed, if $\rho_f = \rho_s$, then mass conservation is automatic, the fluid and solid velocities on the interface are equal, and as a consequence $\boldsymbol{h} \cdot \boldsymbol{n} = 0$ on Γ. It is worth remarking that, $g^{(0)} = 0$ does not imply $\tilde{g}^{(0)} = 0$: the interface moves in absence of a density difference, with leading-order velocity driven by $\tilde{g}^{(0)}$ and provided by equation (5.11). The assumption (5.42) applies in most applications of interest, for example interstitial fluid versus cells in biological tissues, or water versus ice in glaciers.

Whenever (5.42) does not apply and there is a density jump between the solid and fluid phases, possible choices for the growth law $\tilde{g}^{(0)}$ are restricted by the compatibility condition (5.40). For example, any functional form of $\tilde{g}^{(0)}$ that takes the form

$$\tilde{g}^{(0)} = \boldsymbol{v}^* \cdot \boldsymbol{n} \qquad (5.43)$$

satisfies the compatibility condition (5.40) provided that $\boldsymbol{v}^*$ is a locally divergence-free vector field,

$$\nabla_{\boldsymbol{y}} \cdot \boldsymbol{v}^* = 0 \text{ in } \Omega_f. \qquad (5.44)$$

Clearly, a prescription of the type (5.43) is in general time-dependent because $\boldsymbol{n}$ evolves in time while the interface is moving. In practice in this scenario, given a suitable initial condition on the interface position, it suffices to prescribe the velocity field $\boldsymbol{v}^*$ (satisfying (5.44)); from here the updated interface normal vector $\boldsymbol{n}$ may be calculated using the leading-order kinematics of the interface (5.10) for every $t \in (0, T)$.

5.2 *Effective poroelasticity*

Finally, we require a set of macroscale equations to close the system for the solid displacement $\boldsymbol{u}^{(0)}$ and the fluid pressure $p^{(0)}$. Taking the integral average of the sum of (5.12) and (5.18) and using the divergence theorem yields

$$\frac{1}{|\Omega|} \int_{\Gamma} \left(\sigma^{(1)} \boldsymbol{n} - \tau^{(1)} \boldsymbol{n} \right) \mathrm{d}S_y = \left\langle \nabla_{\boldsymbol{x}} \cdot \tau^{(0)} \right\rangle_s - \phi \nabla_{\boldsymbol{x}} p^{(0)}, \qquad (5.45)$$

where the contributions from the periodic boundaries cancel and the knowledge that $p^{(0)}$ is locally constant has been exploited. Given the normal stress condition on internal boundaries (5.15), (5.45) reduces to:

$$\left\langle \nabla_{\boldsymbol{x}} \cdot \tau^{(0)} \right\rangle_s - \phi \nabla_{\boldsymbol{x}} p^{(0)} = 0. \tag{5.46}$$

Equation (5.46) can be rewritten in terms of $\left\langle \tau^{(0)} \right\rangle_s$ by means of the Reynolds transport theorem (see for example (**6**)) and using $\boldsymbol{y}$-periodicity, namely:

$$\int_{\Omega_s} \nabla_{\boldsymbol{x}} \cdot \tau^{(0)} \, \mathrm{d}\boldsymbol{y} = \nabla_{\boldsymbol{x}} \cdot \int_{\Omega_s} \tau^{(0)} \, \mathrm{d}\boldsymbol{y} + \int_{\Gamma} \tau^{(0)} \boldsymbol{q} \, \mathrm{dS}_y, \tag{5.47}$$

where the vector $\boldsymbol{q}$, which accounts for macroscale variations in the interface Γ, is defined by

$$\boldsymbol{q} := (\nabla_{\boldsymbol{x}} \boldsymbol{r}(\boldsymbol{x}, \boldsymbol{y}, t))^{\mathsf{T}} \boldsymbol{n}. \tag{5.48}$$

Here the fact that the unit outward normal vector to $\partial \Omega_s$ is $-\boldsymbol{n}$ has been used in the simplification. The vector $\boldsymbol{r}$ (see Figure 2), which spans the interface Γ, should be recovered by integration of the interface descriptor (5.10). When each Ω_k is independent of the macroscale, $\boldsymbol{q} = 0$ and we say that the medium is *macroscopically uniform*. Using (5.46) together with (5.47) we obtain:

$$\nabla_{\boldsymbol{x}} \cdot \left\langle \tau^{(0)} \right\rangle_s - \phi \nabla_{\boldsymbol{x}} p^{(0)} + \boldsymbol{s}_\tau = 0, \tag{5.49}$$

where

$$\boldsymbol{s}_\tau := \frac{1}{|\Omega|} \int_{\Gamma} \tau^{(0)} \boldsymbol{q} \, \mathrm{dS}_y \tag{5.50}$$

is the momentum production due to macroscopic changes in the solid-fluid interface.

Now we notice that (5.5, 5.8, 5.19) form a linear Neumann-type differential problem for $\boldsymbol{u}^{(1)}$ which can be written, enforcing (5.20, 5.21), as follows:

$$\nabla_{\boldsymbol{y}} \cdot \left(\mathbb{C} \nabla_{\boldsymbol{y}} \boldsymbol{u}^{(1)} \right) = 0 \qquad \text{in } \Omega_s \tag{5.51}$$

$$\left(\mathbb{C} \nabla_{\boldsymbol{y}} \boldsymbol{u}^{(1)} + \mathbb{C} \nabla_{\boldsymbol{x}} \boldsymbol{u}^{(0)} \right) \boldsymbol{n} = -p^{(0)} \boldsymbol{n} \quad \text{on } \Gamma, \tag{5.52}$$

equipped with $\boldsymbol{y}$-periodicity in Ω_s. Since $\boldsymbol{u}^{(1)}$ is guaranteed to be a bounded vector function of $\boldsymbol{y}$ by local periodicity, then the solution is found to be unique up to an arbitrary $\boldsymbol{y}$-constant vector field and can be expressed, exploiting linearity of the problem, as:
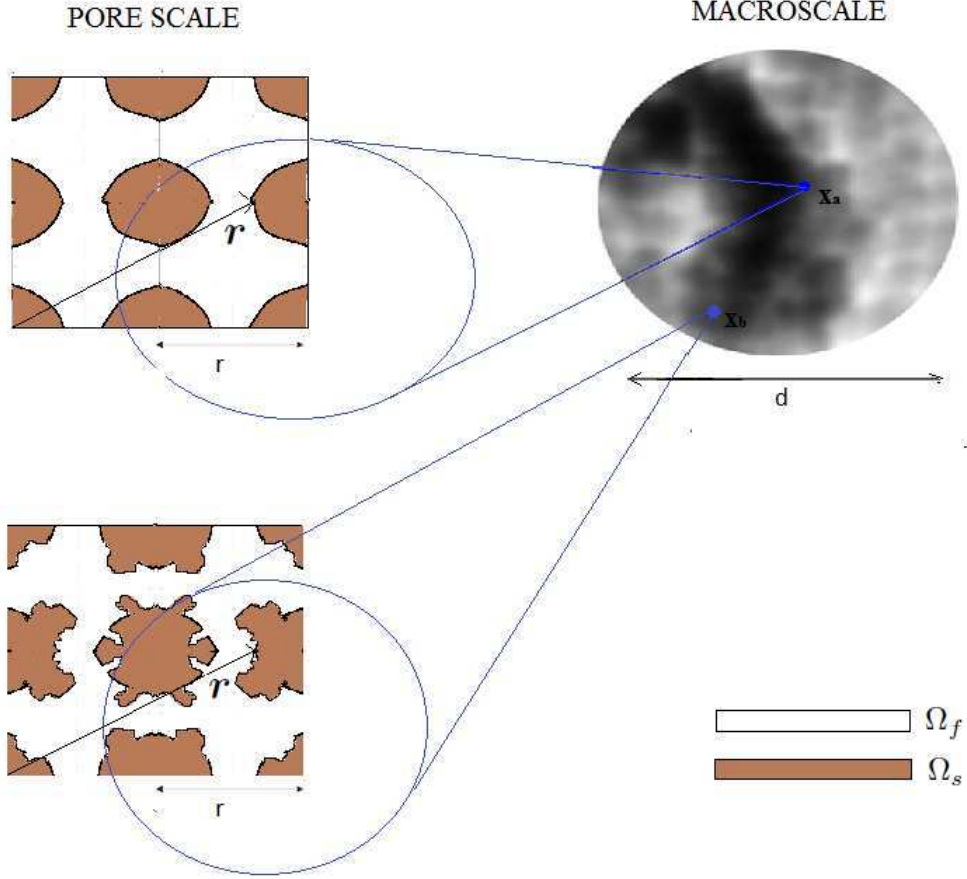
$$\boldsymbol{u}^{(1)} = \mathcal{A} \nabla_{\boldsymbol{x}} \boldsymbol{u}^{(0)} + \boldsymbol{a} p^{(0)}, \tag{5.53}$$

where $\mathcal{A}$ is a rank three tensor, with components denoted A_{ijk} for $i, j, k = 1, 2, 3$.

The cell problem for the vector $\boldsymbol{a}$ is given by:

$$\nabla_{\boldsymbol{y}} \cdot (\mathbb{C} \nabla_{\boldsymbol{y}} \boldsymbol{a}) = 0 \qquad \text{in } \Omega_s \tag{5.54}$$

$$(\mathbb{C} \nabla_{\boldsymbol{y}} \boldsymbol{a}) \boldsymbol{n} = -\boldsymbol{n} \qquad \text{on } \Gamma, \tag{5.55}$$

Fig. 2 2D schematic of a non-macroscopically uniform medium. In this case, the model supports macroscale variations of the microstructure so that, for every fixed $t \in (0, T)$, the interface position vector $\boldsymbol{r}$ related to the same (homologous by $\boldsymbol{y}$-periodicity) local point is varying with respect to $\boldsymbol{x}$, that is $\boldsymbol{r}(\boldsymbol{x_a}, \boldsymbol{y}, t) \neq \boldsymbol{r}(\boldsymbol{x_b}, \boldsymbol{y}, t)$. Whenever the medium exhibits such variations, one cell problem for every $\boldsymbol{x}$ of the homogenised domain needs to be solved.

whereas $\mathcal{A}$ satisfies, in component notation:

$$\frac{\partial}{\partial y_j} \left(C_{ijkl} \frac{\partial A_{k\nu\gamma}}{\partial y_l} \right) = 0 \quad \text{in } \Omega_s \tag{5.56}$$

$$C_{ijkl} \frac{\partial A_{k\nu\gamma}}{\partial y_l} n_j + C_{ij\nu\gamma} n_j = 0 \quad \text{on } \Gamma, \tag{5.57}$$

where $i, j, k, l, \nu, \gamma = 1...3$ and summation over repeated notation indices is used.

As previously, a further condition for $\boldsymbol{a}$ and each A_{ijk} is required to ensure uniqueness;

example conditions are:

$$\langle \boldsymbol{a} \rangle_s = 0, \quad \langle A_{ijk} \rangle_s = 0 \;\; \forall \; i, j, k = 1...3. \tag{5.58}$$

Note that, since $\boldsymbol{u}^{(1)}$ is directly related to the leading order solid stress tensor via (5.19), the form of $\boldsymbol{u}^{(1)}$ given by (5.53) indicates that $\tau^{(0)}$ (and also its cell average) is a function of both the gradient of the leading order solid displacement and the macroscopic fluid pressure $p^{(0)}$, as expected for a poroelastic material. In fact, enforcing equation (5.53), we can exploit equation (5.19), which relates the leading order solid stress tensor to $\nabla_{\boldsymbol{x}} \boldsymbol{u}^{(0)}$ and $\nabla_{\boldsymbol{y}} \boldsymbol{u}^{(1)}$, to provide an explicit relationship for $\tau^{(0)}$ as a function of $\nabla_{\boldsymbol{x}} \boldsymbol{u}^{(0)}$ and $p^{(0)}$, namely:

$$\tau^{(0)} = (\mathbb{C}\mathbb{M} + \mathbb{C}) \, \nabla_{\boldsymbol{x}} \boldsymbol{u}^{(0)} + \mathbb{C}\mathsf{Q} p^{(0)}, \tag{5.59}$$

where the fourth rank tensor $\mathbb{M}$ and the second rank tensor Q are defined as follows:

$$\mathbb{M} := \nabla_{\boldsymbol{y}} \mathcal{A}, \quad \mathsf{Q} := \nabla_{\boldsymbol{y}} \boldsymbol{a}. \tag{5.60}$$

Now, (5.49-5.50) can be regarded as the effective macroscale stress equilibrium equations for the poroelastic medium.

A final scalar equation is required to close the macroscale model for the zeroth order variables $\boldsymbol{u}^{(0)}$, $\langle \boldsymbol{v}^{(0)} \rangle_f$, $p^{(0)}$ and this is provided by averaging the incompressibility condition (5.14) to give:

$$\left\langle \nabla_{\boldsymbol{y}} \cdot \boldsymbol{v}^{(1)} \right\rangle_f + \left\langle \nabla_{\boldsymbol{x}} \cdot \boldsymbol{v}^{(0)} \right\rangle_f = 0. \tag{5.61}$$

Applying the divergence theorem in the $\boldsymbol{y}$ variable, $\boldsymbol{y}$-periodicity together with equation (5.17), and the Reynolds theorem in $\boldsymbol{x}$ gives:

$$\frac{1}{|\Omega|} \int_{\Gamma} \dot{\boldsymbol{u}}^{(1)} \cdot \boldsymbol{n} \; \mathrm{d}S_y + \nabla_{\boldsymbol{x}} \cdot \left\langle \boldsymbol{v}^{(0)} \right\rangle_f - s_{\mathrm{v}} = 0 \tag{5.62}$$

where

$$s_{\mathrm{v}} := \frac{1}{|\Omega|} \int_{\Gamma} (\boldsymbol{v}^{(0)} \cdot \boldsymbol{q} - g^{(1)}) \; \mathrm{d}S_y \tag{5.63}$$

is an effective mass source which is related to both the lack of macroscopic uniformity and to surface accretion (through $g^{(1)}$). Since

$$\int_{\Gamma} \dot{\boldsymbol{u}}^{(1)} \cdot \boldsymbol{n} \; \mathrm{d}S_y = - \int_{\Omega_s} \nabla_{\boldsymbol{y}} \cdot \dot{\boldsymbol{u}}^{(1)} \; \mathrm{d}\boldsymbol{y} = - \int_{\Omega_s} \mathrm{Tr} \left(\nabla_{\boldsymbol{y}} \dot{\boldsymbol{u}}^{(1)} \right) \mathrm{d}\boldsymbol{y}, \tag{5.64}$$

equation (5.62) can be rewritten by means of (5.53) and (5.60), accounting for (5.20, 5.21), as follows:

$$\nabla_{\boldsymbol{x}} \cdot \left\langle \boldsymbol{v}^{(0)} \right\rangle = \left\langle \mathrm{Tr} \, \dot{\mathbb{M}} \right\rangle_s : \nabla_{\boldsymbol{x}} \boldsymbol{u}^{(0)} + \left\langle \mathrm{Tr} \, \mathbb{M} \right\rangle_s : \nabla_{\boldsymbol{x}} \dot{\boldsymbol{u}}^{(0)} + \left\langle \mathrm{Tr} \, \dot{\mathsf{Q}} \right\rangle_s p^{(0)} + \left\langle \mathrm{Tr} \, \mathsf{Q} \right\rangle_s \dot{p}^{(0)} + s_{\mathrm{v}} \tag{5.65}$$

Having derived the new effective model on the macroscale, in the next sections we discuss the physical relevance of the various terms before comparing it against traditional poroelastic frameworks in the literature.

6. Discussion of the results

We have derived the homogenised macroscale model for the mechanical behaviour of a poroelastic medium, incorporating surface growth of the solid phase (provided that a suitable growth law is imposed constitutively). Equations (5.37, 5.49, 5.65) form the effective macroscale differential system to be solved for a growing poroelastic medium, provided that the time evolution of the microstructure is updated by (5.10-5.11). It is a closed system for the leading order fields $\left\langle \boldsymbol{v}^{(0)} \right\rangle_f$, $\boldsymbol{u}^{(0)}$, $p^{(0)}$, which are functions of $\boldsymbol{x}$ and t only; substituting (5.27) and (5.59) into (5.49), (5.65) yields a self-consistent system of partial differential equations for the leading order displacement and pressure fields $\boldsymbol{u}^{(0)}$ and $p^{(0)}$, so that the average fluid velocity $\left\langle \boldsymbol{v}^{(0)} \right\rangle_f$ can be finally recovered by means of (5.37).

The macroscale behavior of the fluid flow is given by an effective Darcy-type law for the relative average velocity $\left\langle \dot{\boldsymbol{w}} \right\rangle_f = \left\langle \boldsymbol{v}^{(0)} \right\rangle_f - \phi \dot{\boldsymbol{u}}^{(0)}$ given by (5.37). The effective permeability tensor $\left\langle \tilde{\mathsf{W}} \right\rangle_f (\boldsymbol{x}, t)$ provides the link between macroscale fluid transport and the pore-scale geometry and dynamics. The correction velocity $\left\langle \boldsymbol{h} \right\rangle_f$ on the left hand side of (5.37) comes from global mass conservation (the solid and fluid phases exchange mass without any surface source), and vanishes whenever there is no density difference between the two compartments.

The effective stress equilibrium equations (5.49) can be written in the form:

$$\nabla_{\boldsymbol{x}} \cdot \tau_E = -\boldsymbol{s}_\tau, \tag{6.1}$$

where

$$\tau_E := \left\langle \tau^{(0)} \right\rangle_s - \phi p^{(0)} \mathsf{I} = \left\langle \mathbb{C}\mathbb{M} + \mathbb{C} \right\rangle_s \nabla_{\boldsymbol{x}} \boldsymbol{u}^{(0)} + \left(\left\langle \mathbb{C}\mathsf{Q} \right\rangle_s - \phi \mathsf{I} \right) p^{(0)}. \tag{6.2}$$

Equations (6.1) and (6.2) can be formally viewed as the average force balance equations for the poroelastic medium.

The scalar equation (5.65), which in standard poroelasticity directly relates the pressure to the fluid and solid phases motion, here encodes instead both the surface growth and the movement of the material. The two terms on the right hand side, including time derivatives of the fields $p^{(0)}$ and $\boldsymbol{u}^{(0)}$, are related to the small displacement of the structure. The two terms including the time derivatives of the coefficients (Tr $\dot{\mathbb{M}}$, Tr $\dot{\mathsf{Q}}$) account for the interplay between the elastic movement of the structure and surface growth. In fact, they reduce to zero both in the no growth limit (the coefficients are no longer varying in time) and in the rigid limit (every $\boldsymbol{u}^{(l)}$ for $l = 0, 1, \ldots$ reduces to zero, implying that, through (5.53) and (5.60), $\mathsf{Q} = 0$).

REMARK 6.1. Since the interface Γ is moving, it should be understood that every cell problem must be solved in the evolving geometry, described by the leading-order equation for transport of the interface (5.10). As a result, the cell variables $\tilde{\mathsf{W}}$, $\boldsymbol{P}$, $\boldsymbol{h}$, p_h, $\mathcal{A}$, $\boldsymbol{a}$ are microscale variables, and depend on t as well as $\boldsymbol{x}$. Hence, although the effect of growth is purely geometrical at the microscale, it impacts on the macroscale model through the dependence of such variables on the microscale geometry. This represents a crucial difference

compared to previous works, where the cell problems and the related macroscale coefficients do not involve any time dependence (see for example (**33**) and (**36**)).

REMARK 6.2. When the elasticity tensor $\mathbb{C}$ is $\boldsymbol{y}$-constant, the unique (up to a $\boldsymbol{y}$-constant vector field) solution of (5.51-5.52) can be written in the form:

$$\boldsymbol{u}^{(1)} = \mathcal{A}\nabla_{\boldsymbol{x}}\boldsymbol{u}^{(0)} + \boldsymbol{a}p^{(0)} = \tilde{\mathcal{A}}\mathbb{C}\nabla_{\boldsymbol{x}}\boldsymbol{u}^{(0)} + \boldsymbol{a}p^{(0)}, \tag{6.3}$$

where the three-rank tensor $\tilde{\mathcal{A}}$ solves, componentwise:

$$\frac{\partial}{\partial y_j}\left(C_{ijkl}\frac{\partial \tilde{A}_{k\nu\gamma}}{\partial y_l}\right) = 0 \quad \text{in } \Omega_s \tag{6.4}$$

$$C_{ijkl}\frac{\partial \tilde{A}_{k\nu\gamma}}{\partial y_l}n_j + \delta_{i\nu}\delta_{j\gamma}n_j = 0 \quad \text{on } \Gamma. \tag{6.5}$$

Hence, defining the tensor:

$$\mathbb{L} := \nabla_{\boldsymbol{y}}\tilde{\mathcal{A}} \tag{6.6}$$

yields

$$\nabla_{\boldsymbol{y}}\boldsymbol{u}^{(1)} = \mathbb{M}\nabla_{\boldsymbol{x}}\boldsymbol{u}^{(0)} + \mathsf{Q}p^{(0)} = \mathbb{L}\mathbb{C}\nabla_{\boldsymbol{x}}\boldsymbol{u}^{(0)} + \mathsf{Q}p^{(0)}, \tag{6.7}$$

so that $\mathbb{M} = \mathbb{L}\mathbb{C}$. Furthermore, comparing (6.4-6.5) with the cell problem for $\boldsymbol{a}$ given by (5.54-5.55), we deduce that

$$\text{Tr}\,\tilde{\mathcal{A}} = \boldsymbol{a}, \tag{6.8}$$

or, in component notation,

$$\tilde{A}_{ikk} = a_i, \quad i = 1...3, \tag{6.9}$$

up to an $\boldsymbol{y}$-constant vector.

In summary, in the simplified scenario of a locally constant elasticity tensor, once $\tilde{\mathcal{A}}$ is calculated solving the cell problem (6.4-6.5), it suffices to exploit (6.9) to obtain the vector $\boldsymbol{a}$ and hence the tensors Q and $\mathbb{L}$ via (5.60) and (6.6).

6.1 Macroscopic uniformity

The momentum source $\boldsymbol{s}_\tau$ and the mass source s_{v} are both related to variations of the interface position vector $\boldsymbol{r}$ with respect to $\boldsymbol{x}$; these contributions arise when a poroelastic growing medium is not macroscopically uniform, so that $\Omega_k = \Omega_k(\boldsymbol{x}, \boldsymbol{y})$ and in particular $\boldsymbol{q} \neq 0$. The vector $\boldsymbol{q}$ reduces to zero whenever $\boldsymbol{r} = \boldsymbol{r}(\boldsymbol{y}, t)$ only and this implies, in turn, that both the initial value for the interface position and the interface velocity are $\boldsymbol{x}$-constant, so that:

$$F_0^{(0)} = F_0^{(0)}(\boldsymbol{y}), \tag{6.10}$$

$$\boldsymbol{v}_\Gamma^{(0)} = \boldsymbol{v}_\Gamma^{(0)}(\boldsymbol{y}, t), \quad \forall t \in (0, T), \tag{6.11}$$

where $F_0^{(0)} = F^{(0)}|_{t=0}$. However, the interface velocity is directly related to the growth law $\tilde{g}$ (see equation 2.16), so that, since we have assumed that movement of the interface is dominated by surface accretion, condition (6.11) is equivalent to:

$$\tilde{g}^{(0)} = \tilde{g}^{(0)}(\boldsymbol{y}, t) \quad \forall t \in (0, T). \tag{6.12}$$

Whenever the medium is macroscopically uniform $\boldsymbol{s}_\tau$ and s_v simplify to:

$$\boldsymbol{s}_\tau = 0, \tag{6.13}$$

$$s_\mathrm{v} = -\frac{1}{|\Omega|} \int_\Gamma g^{(1)}(\boldsymbol{y}, t) \, \mathrm{dS}_y, \tag{6.14}$$

and the macroscale model to be solved becomes

$$\begin{cases} \left\langle \boldsymbol{v}^{(0)} \right\rangle_f - \phi \dot{\boldsymbol{u}}^{(0)} = -\left\langle \tilde{\mathsf{W}} \right\rangle_f \nabla_{\boldsymbol{x}} p^{(0)} + \langle \boldsymbol{h} \rangle_f \, , \\ \nabla_{\boldsymbol{x}} \cdot \tau_E = 0, \\ \nabla_{\boldsymbol{x}} \cdot \left\langle \boldsymbol{v}^{(0)} \right\rangle_f = \left\langle \mathrm{Tr} \, \dot{\mathbb{M}} \right\rangle_s : \nabla_{\boldsymbol{x}} \boldsymbol{u}^{(0)} + \langle \mathrm{Tr} \, \mathbb{M} \rangle_s : \nabla_{\boldsymbol{x}} \dot{\boldsymbol{u}}^{(0)} + \left\langle \mathrm{Tr} \, \dot{\mathsf{Q}} \right\rangle_s p^{(0)} + \langle \mathrm{Tr} \, \mathsf{Q} \rangle_s \dot{p}^{(0)} + s_\mathrm{v}, \end{cases} \tag{6.15}$$

where (6.2) represents the effective constitutive relationship for the poroelastic growing medium.

Whenever macroscopic uniformity applies, the following solution scheme for the macroscale model applies:

1. Fix material properties of the medium ρ_s, ρ_f, μ, and elastic moduli $\mathbb{C}$.
2. Fix a microscale structure, including a unit cell definition together with an initial value for the interface position $F_0^{(0)}(\boldsymbol{y})$.
3. Prescribe constitutively a growth law $\tilde{g}$, so that every $\tilde{g}^{(l)}$ for $l = 0, 1...$ is defined. In particular, $g^{(0)}$ must satisfy the compatibility condition (5.40). Whenever the densities of the solid and fluid phases are equal ($\rho_s = \rho_f$), every $g^{(l)} = 0$ for $l = 0, 1, \ldots$ so the compatibility condition (5.40) is automatic and $\boldsymbol{h} = \boldsymbol{0}$.
4. Fix a macroscale geometry and corresponding boundary conditions.
5. Solve the cell problems (5.29-5.30), (5.32-5.33), (5.54-5.55), (5.56-5.57) and calculate the corresponding macroscale model coefficients exploiting (5.1) and (5.60).
6. Solve the macroscale model (6.15), using (6.2) as the effective constitutive relationship for the material.
7. Update the interface position by means of equation (5.10), where the leading-order interface velocity is recovered by relationship (5.11).
8. Repeat the calculations explained in (5,6,7) for every $t \in (0, T)$.

It is worth remarking that, whenever the medium is not macroscopically uniform, additional momentum and mass sources of the form (5.50, 5.63) must be taken into account. Further, the interface position would depend on the macroscale variable $\boldsymbol{x}$, so that, in principle, every cell problem should be solved for each $\boldsymbol{x}$ belonging to the macroscale domain (see Figure 2). Hence, in this scenario, computational feasibility may be compromised.

7. Particular cases

In this section we focus on specific physical regimes, namely the no-growth limit and the macroscopic isotropy of the poroelastic material. These particular cases are chosen as they coincide with traditional literature results, namely the standard poroelasticity models of Burridge and Keller (**29**), and also a physically-relevant special case.

In order to avoid unessential technicalities and to better highlight the results, in the following we assume that $\mathbb{C}$ is $\boldsymbol{y}$-constant, so that the considerations in Remark 6.2 apply.

7.1 *No growth limit and comparison with standard poroelasticity*

In the limiting case of no growth, we compare our model to the classical poroelasticity results. In particular, we refer to (**29**), where the authors derive a set of equations for a poroelastic medium by means of a multiscale approach, that matches the classical Biot's system of equations, reported in (**30**) and (**31**), in the case of macroscopic uniformity.

Thus, setting $\tilde{g} = 0$ and $\boldsymbol{q} = 0$ our results, written for the average relative fluid-solid velocity $\langle \dot{\boldsymbol{w}} \rangle_f$, the leading order elastic displacement $\boldsymbol{u}^{(0)}$ and the leading order pressure $p^{(0)}$, reduce to:

$$
\begin{cases}
\langle \dot{\boldsymbol{w}} \rangle_f = - \left\langle \tilde{\mathsf{W}} \right\rangle_f \nabla_{\boldsymbol{x}} p^{(0)} & (7.1) \\[2mm]
\nabla_{\boldsymbol{x}} \cdot \left\langle \tau^{(0)} \right\rangle_s - \phi \nabla_{\boldsymbol{x}} p^{(0)} = 0 & (7.2) \\[2mm]
\dot{p}^{(0)} = \dfrac{1}{\langle \mathrm{Tr}\, \mathsf{Q} \rangle_s} \left[\mathrm{Tr} \left(\phi \nabla_{\boldsymbol{x}} \dot{\boldsymbol{u}}^{(0)} - \left\langle \mathbb{L}\mathbb{C} \nabla_{\boldsymbol{x}} \dot{\boldsymbol{u}}^{(0)} \right\rangle_s \right) + \nabla_{\boldsymbol{x}} \cdot \langle \dot{\boldsymbol{w}} \rangle_f \right] & (7.3) \\[2mm]
\left\langle \tau^{(0)} \right\rangle_s = \langle \mathbb{C}\mathbb{L}\mathbb{C} + \mathbb{C} \rangle_s \nabla_{\boldsymbol{x}} \boldsymbol{u}^{(0)} + \langle \mathbb{C}\mathsf{Q} \rangle_s \, p^{(0)}, & (7.4)
\end{cases}
$$

where in (7.3) terms have been rearranged and the interface is assumed fixed, so that the coefficients are no longer varying in time. Since we are in a linearized motion context and the subdomains Ω_f and Ω_s are no longer time dependent, following (**29**), we focus on linearized dynamics. We consider time harmonic motion with angular frequency ω, such that for every field ψ we have:

$$
\dot{\psi} = i\omega\psi. \qquad (7.5)
$$

Then (7.1-7.3) become

$$
\begin{cases}
\langle \boldsymbol{w} \rangle_f = - \langle \mathsf{W} \rangle_f \nabla_{\boldsymbol{x}} p^{(0)} & (7.6) \\[2mm]
\nabla_{\boldsymbol{x}} \cdot \left\langle \tau^{(0)} \right\rangle_s - \phi \nabla_{\boldsymbol{x}} p^{(0)} = 0 & (7.7) \\[2mm]
p^{(0)} = \dfrac{1}{\langle \mathrm{Tr}\, \mathsf{Q} \rangle_s} \left[\phi \nabla_{\boldsymbol{x}} \cdot \boldsymbol{u}^{(0)} - \mathrm{Tr} \langle \mathbb{L}\mathbb{C} \rangle_s : \nabla_{\boldsymbol{x}} \boldsymbol{u}^{(0)} + \nabla_{\boldsymbol{x}} \cdot \langle \boldsymbol{w} \rangle_f \right], & (7.8)
\end{cases}
$$

where $\mathsf{W} = \dfrac{1}{i\omega}\tilde{\mathsf{W}}$ solves

$$
i\omega\mu \nabla_{\boldsymbol{y}}^2 \mathsf{W}^{\mathsf{T}} - \nabla_{\boldsymbol{y}} \boldsymbol{P} + \mathsf{I} = 0 \quad \text{in } \Omega_f \qquad (7.9)
$$

$$
\nabla_{\boldsymbol{y}} \cdot \mathsf{W}^{\mathsf{T}} = 0 \quad \text{in } \Omega_f \qquad (7.10)
$$

$$
\mathsf{W} = 0 \quad \text{on } \Gamma. \qquad (7.11)
$$

This system recovers the results of (**29**) [†], when they are simplified to the quasistatic scenario. Furthermore, the scalar coefficient multiplying the square brackets in (7.8), which is, in the present framework, directly related to the geometric and mechanical properties of

---

[†] Equations (7.4,7.6-7.8) are equivalent to (36a, 39a, 39b, 36b), page 1443, (**29**), where average quantities are represented by the superscript $^-$ instead of brackets $\langle \rangle$ and the porosity is denoted by V_f instead of ϕ.

the elastic phase only, should be compared to the one in $(\mathbf{29})^{\ddagger}$ given, in our notation, by

$$-\frac{\kappa}{\phi - \kappa \langle \operatorname{Tr} \mathsf{Q} \rangle_s}, \tag{7.12}$$

where κ denotes the bulk modulus. Since incompressibility of the fluid phase is assumed here,

$$\lim_{\kappa \to \infty} \left(-\frac{\kappa}{\phi - \kappa \langle \operatorname{Tr} \mathsf{Q} \rangle_s} \right) = \frac{1}{\langle \operatorname{Tr} \mathsf{Q} \rangle_s}, \tag{7.13}$$

and hence standard poroelasticity is recovered. Note that, as in $(\mathbf{29})$, if the solid matrix is rigid, $\boldsymbol{u}^{(l)} = 0$ for every l, $\dot{\boldsymbol{w}} = \boldsymbol{v}^{(0)}$ and $\mathsf{Q} = 0$. Thus rearranging terms, equations (7.6,7.8) are sufficient to close the system for $(\boldsymbol{v}^{(0)}, p^{(0)})$, which reduces to:

$$\begin{cases} \left\langle \boldsymbol{v}^{(0)} \right\rangle_f = -\left\langle \tilde{\mathsf{W}} \right\rangle_f \nabla_{\boldsymbol{x}} p^{(0)} & (7.14) \\[2mm] \nabla_{\boldsymbol{x}} \cdot \left\langle \boldsymbol{v}^{(0)} \right\rangle_f = 0, & (7.15) \end{cases}$$

so that we recover the simple incompressible Darcy's flow when a rigid, non-growing solid phase is assumed.

REMARK 7.1. In this work we assume quasistatic dynamical conditions and incompressibility of the fluid phase, a restriction with respect to the regime addressed in $(\mathbf{29})$. These assumptions can be easily relaxed but add no increased physical insight. Moreover, we assume local periodicity, whereas in $(\mathbf{29})$ every field is simply a bounded function of $\boldsymbol{y}$. Our formulation can nevertheless be generalized to local boundness, when assuming that $\Gamma = \partial \Omega_s = \partial \Omega_f$. In this case, the results would be formally equivalent, but substantially different, because the resulting microscale differential problems would not be *cell*-decoupled problems and they would have to be solved on the whole microscale domain. It is worth remarking that the present formulation allows us to account for arbitrary macroscale boundary conditions, the latter prescribed, for example, by another mechanical system interacting with the poroelastic growing medium.

7.2 *Macroscopically isotropic medium*

When the poroelastic medium is macroscopically isotropic, we obtain

$$\left\langle \tilde{\mathsf{W}} \right\rangle_f = \frac{\mathsf{k}}{\mu} \mathsf{I} \tag{7.16}$$

$$\langle \operatorname{Tr} \mathbb{L}\mathbb{C} \rangle_s = \alpha \mathsf{I} \tag{7.17}$$

$$\langle \mathsf{Q} \rangle_s = \beta \mathsf{I} \rightarrow \langle \operatorname{Tr} \mathsf{Q} \rangle_s = 3\beta \tag{7.18}$$

$$\langle \mathbb{C}\mathbb{L}\mathbb{C} + \mathbb{C} \rangle_s \nabla_{\boldsymbol{x}} \boldsymbol{u}^{(0)} = \lambda \nabla_{\boldsymbol{x}} \cdot \boldsymbol{u}^{(0)} \mathsf{I} + 2\hat{\mu} \mathsf{e}^{(0)}, \tag{7.19}$$

---

‡ We refer to equations (36b,37), page 1443, $(\mathbf{29})$

where

$$\mathsf{e}^{(0)} := \frac{1}{2}\left[\nabla_{\boldsymbol{x}}\boldsymbol{u}^{(0)} + (\nabla_{\boldsymbol{x}}\boldsymbol{u}^{(0)})^{\mathsf{T}}\right],$$

and k, λ, $\hat{\mu}$ formally play the role of an effective permeability and Lamé constants respectively, whereas α and β are poroelastic parameters. Note that α, λ, β and $\hat{\mu}$ depend both on the evolving microstructure and on the microscale elastic properties of the medium, whereas k is purely geometric and, in general, all of them are functions of $\boldsymbol{x}$ and t. Following Remark 6.2, we adapt results (5.37,5.49,5.65) accordingly and exploit (7.16-7.19), so that, for a macroscopically isotropic poroelastic growing medium, the system of equations to be solved reads:

$$\begin{cases} \left\langle \boldsymbol{v}^{(0)} \right\rangle_f - \phi\dot{\boldsymbol{u}}^{(0)} = -\frac{\mathsf{k}}{\mu}\nabla_{\boldsymbol{x}}p^{(0)} + \left\langle \boldsymbol{h} \right\rangle_f & (7.20) \\[2mm] \nabla_{\boldsymbol{x}} \cdot \tau_E = -\boldsymbol{s}_\tau & (7.21) \\[2mm] \nabla_{\boldsymbol{x}} \cdot \left\langle \boldsymbol{v}^{(0)} \right\rangle_f = \dot{\alpha}\nabla_{\boldsymbol{x}} \cdot \boldsymbol{u}^{(0)} + \alpha\nabla_{\boldsymbol{x}} \cdot \dot{\boldsymbol{u}}^{(0)} + 3\dot{\beta}p^{(0)} + 3\beta\dot{p}^{(0)} + s_{\mathrm{v}}, & (7.22) \end{cases}$$

while the effective isotropic constitutive relationship is:

$$\tau_E := \left[\lambda\nabla_{\boldsymbol{x}} \cdot \boldsymbol{u}^{(0)} + (\alpha - \phi)p^{(0)}\right]\mathsf{I} + 2\hat{\mu}\mathsf{e}^{(0)}. \tag{7.23}$$

8. Conclusions

We have developed a theoretical model which describes the macroscopic behaviour of a poroelastic medium, when surface mass exchange occurs in the pores. The starting point is a coupled description of linear elasticity and Stokes' flow of the solid and fluid phases at the pore-scale. The solid and fluid mechanics are coupled through continuity of stress and mass flow on the displacing solid-fluid interface. Next, homogenisation via multiple scales yields the effective model on the macroscale. The result is a new system of equations for a poroelastic medium where time-dependent growth is encoded in the coefficients of the model; these coefficients can be computed by solving cell problems on the evolving microstructure.

The fluid flow is described through a Darcy-type law (5.37) for the relative average velocity of the fluid and solid phase, with an associated permeability tensor that captures the dependence on the pore-scale structure. A correction velocity $\langle \boldsymbol{h} \rangle_f$ appears as a consequence of the global transfer of mass between the solid and fluid phases. The mechanical properties of the poroelastic growing medium are directly encoded in a new effective constitutive relationship (5.59) which accounts for the fluid pressure in the pore, small elastic displacement of the structure and surface accretion of the solid phase. The interplay between the strain of the structure and appositional growth resides in the effective mass source contributions.

When macroscopic uniformity applies, the model simplifies and a solution strategy is provided. Limiting cases of the model are explored: in absence of growth, the model reduces to the classical result of Burridge and Keller (**29**), while the assumption of isotropic growth leads to a much simpler set of equations. In the latter scenario, hydraulic and mechanical parameters are recovered, which formally play the role of effective permeability and Lamé

moduli, respectively. A distinction can be made between parameters which depend purely on the evolving microstructure and pore scale elastic properties of the medium, and those which are purely geometric.

The homogenised set of equations has been obtained under assumption of periodic microstructure, infinitesimal strain and slow flow. While a slow modulation of the periodicity could be introduced without affecting the main results, the physical assumptions underlying the use of linear elasticity and Stokes' equations cannot be relaxed.

There are numerous opportunities for extension and application of the model presented here to specific mechanical systems. A natural development is to compare predictions of our new model to the classical description of Biot in the context of specific pore-scale structures. (In (**38**) the authors account for surface growth of a rigid solid porous medium, and numerical solutions of the resulting model are explored). In general, a critical next step in the application of the models derived here is to introduce constitutive equations for the mass exchange rate $\tilde{g}$, motivated by the specific application under consideration. This will enable simulations to be performed, model testing and prediction.

References

1. Davit, Y., Bell, C., Byrne, H., Chapman, L., Kimpton, L., Lang, G., Leonard, K., Oliver, J., Pearson, N., Shipley, R., Waters, S., Whiteley, J., Wood, B., Quintard, M.: Homogenization via formal multiscale asymptotics and volume averaging: how do the two techniques compare? Advances in Water Resources (in press) (2013)

2. Bowen, R.: Incompressible porous media models by the use of the theory of mixtures. Int. J. Eng. Science **18**, 1129–1148 (1980)

3. Bowen, R.: Compressible porous media models by the use of the theory of mixtures. Int. J. Eng. Science **20**, 697–735 (1982)

4. Sanchez-Palencia, E.: Non-Homogeneous Media and Vibration Theory-Lecture Notes in Physics 127. Springer-Verlag, Berlin, Germany (1980)

5. Sanchez-Palencia, E.: Homogenization method for the study of composite media. Asymptotic analysis II-Lecture notes in mathematics **985**, 192–214 (1983)

6. Holmes, M.: Introduction to perturbation method. Springer-Verlag, Harrisonburg, VA, USA (1995)

7. Mei, C.C., Vernescu, B.: Homogenization Methods for multiscale mechanics. World Scientific, Singapore (2010)

8. Rodriguez, E., Hoger, A., McCulloch, A.: Stress -dependent finite growth in soft elastic tissues. J. Biomech. **27**, 455–467 (1994)

9. Taber, L.: Biomechanics of growth, remodeling and morphogenesis. Appl Mech. Rev. **48**, 487–545 (1995)

10. Ambrosi, D., Guana, F.: Stress–modulated growth. Math Mech. Solids **12**, 319–342 (2007)

11. Ambrosi, D., Vitale, G., Preziosi, L.: The insight of mixtures theory for growth and remodeling. ZAMP **61**, 177–191 (2010)

12. Whitaker, S.: The transport equations for multi-phase systems. Chemical Engineering Science **28**(1), 139–147 (1973)
13. Gray, W.G.: A derivation of the equations for multi-phase transport. Chemical Engineering Science **30**(2), 229–233 (1975)
14. Hutter, K.: Theoretical glaciology: material science of ice and the mechanics of glaciers and ice sheets. Reidel, Dordrecht and Boston and Tokyo, Japan and Hingham, MA (1983)
15. Cowin, S.C.: Tissue growth and remodeling. Annu. Rev. Biomed. Eng. **6**, 77–107 (2004)
16. Ateshian, G.A.: On the theory of reactive mixtures for modeling biological growth. Biomechanics and modeling in mechanobiology **6**(6), 423–445 (2007)
17. Bottaro, A., Ansaldi, T.: On the infusion of a therapeutic agent into a solid tumor modeled as a poroelastic medium. Journal of Biomechanical engineering **134**, 1–6 (2012)
18. Roose, T., Chapman, S.J., Maini, P.K.: Mathematical models of avascular tumor growth. Siam Review **49**(2), 179–208 (2007)
19. Roose, T., Netti, P.A., Munn, L.L., Boucher, Y., Jain, R.K.: Solid stress generated by spheroid growth estimated using a linear poroelasticity model? Microvascular research **66**(3), 204–212 (2003)
20. Moeendarbary, V., Fritzsche, H., Moulding, T., Stride, M., Charras: The cytoplasm of living cells behaves like a poroelastic material. Nature Materials **12**, 253–261 (2013)
21. Bettahalli, N., Vicente, J., Moroni, L., Higuera, G., Van Blitterswijk, C., Wessling, M., Stamatialis, D.: Integration of hollow fiber membranes improves nutrient supply in three-dimensional tissue constructs. Acta biomaterialia **7**(9), 3312–3324 (2011)
22. Humphrey, J., Rajagopal, K.: A constrained mixture model for arterial adaptations to a sustained step change in blood flow. Biomechanics and modeling in mechanobiology **2**(2), 109–126 (2003)
23. Lemon, G., King, J.R., Byrne, H.M., Jensen, O.E., Shakesheff, K.M.: Mathematical modelling of engineered tissue growth using a multiphase porous flow mixture theory. Journal of mathematical biology **52**(5), 571–594 (2006)
24. O'Dea, R.D., Waters, S.L., Byrne, H.M.: A two-fluid model for tissue growth within a dynamic flow environment. European Journal of Applied Mathematics **19**(06), 607–634 (2008)
25. Baek, S., Rajagopal, K., Humphrey, J.: A theoretical model of enlarging intracranial fusiform aneurysms. Journal of Biomechanical Engineering **128**(1), 142–149 (2006)
26. Ciarletta, P., Preziosi, L., Maugin, G.: Mechanobiology of interfacial growth. Journal of the Mechanics and Physics of Solids **61**(3), 852 – 872 (2013)
27. Pioletti, D.P., Rakotomanana, L.R.: Non-linear viscoelastic laws for soft biological tissues. European Journal of Mechanics-A/Solids **19**(5), 749–759 (2000)
28. Preziosi, L., Ambrosi, D., Verdier, C.: An elasto-visco-plastic model of cell aggregates. Journal of Theoretical Biology **262**(1), 35 – 47 (2010)
29. Burridge, R., Keller, J.: Poroelasticity equations derived from microstructure. Journal of acoustical society of America **70**, 1140–1146 (1981)
30. Biot, M.A.: General theory of three-dimensional consolidation. Journal of applied physics **12**(2), 155–164 (1941)
31. Biot, M.A.: Mechanics of deformation and acoustic propagation in porous media. Journal of applied physics **33**(4), 1482–1498 (1962)

32. Mikelic, A., Wheeler, M.F.: On the interface law between a deformable porous medium containing a viscous fluid and an elastic body. Mathematical Models and Method in Applied Sciences **22**, 1–32 (2012)

33. Shipley, R.J., Chapman, J.: Multiscale modelling of fluid and drug transport in vascular tumors. Bulletin of Mathematical Biology. **72**, 1464–1491 (2010)

34. Gurtin, M., Fried, E., Anand, L.: The mechanics and thermodynamics of continua. Cambridge University press, New York, USA (2010)

35. Roose, T., Swartz, M.A.: Multiscale modeling of lymphatic drainage from tissues using homogenization theory. Journal of biomechanics **45**(1), 107–115 (2012)

36. Arbogast, T., Lehr, H.L.: Homogenization of a darcy-stokes system modeling vuggy porous media. Computational Geosciences **10**(3) (2006)

37. Hornung, U.: Homogenization and porous media. Springer, New York, USA (1997)

38. O'Dea, R.D., Nelson, M.R., El Haj, A.J., Waters, S.L., Byrne, H.: A multiscale analysis of nutrient transport and biological tissue growth in vitro. Under submission (2013)

MOX Technical Reports, last issues

Dipartimento di Matematica "F. Brioschi",
Politecnico di Milano, Via Bonardi 9 - 20133 Milano (Italy)

44/2014 PEZZUTO, S.; AMBROSI,D.
Active contraction of the cardiac ventricle and distortion of the microstructural architecture

45/2014 PEZZUTO, S.; AMBROSI,D.; QUARTERONI, A.
An orthotropic active-strain model for the myocardium mechanics and its numerical approximation

46/2014 PENTA, R; AMBROSI, D.
The role of the microvascular tortuosity in tumor transport phenomena

47/2014 PENTA, R; AMBROSI, D; QUARTERONI, A.
Multiscale homogenization for fluid and drug transport in vascularized malignant tissues

48/2014 PENTA, R; AMBROSI, D; SHIPLEY, R.
Effective governing equations for poroelastic growing media

43/2014 BRUGIAPAGLIA, S.; MICHELETTI, S.; PEROTTO, S.
Compressed solving: a numerical approximation technique for PDEs based on compressed sensing

42/2014 CANALE, A.; VANTINI, S.
Constrained Functional Time Series: an Application to Demand and Supply Curves in the Italian Natural Gas Balancing Platform

41/2014 ESFANDIAR, B.; PORTA, G.; PEROTTO, S.; GUADAGNINI, A.
Impact of space-time mesh adaptation on solute transport modeling in porous media

40/2014 ANTONIETTI, P.F.; MAZZIERI, I.; QUARTERONI, A.
Improving seismic risk protection through mathematical modeling

39/2014 GHIGLIETTI, A.; PAGANONI, A.M.
Statistical inference for functional data based on a generalization of Mahalanobis distance